Fatty acid esters of azaspiracids identified in mussels (Mytilus edulis) using liquid chromatography-high resolution mass spectrometry

Mudge, Elizabeth M.; Miles, Christopher O.; Hardstaff, William R.; McCarron, Pearse

National Research Council Canada   Conseil national de recherches Canada

Canada

1   **Fatty Acid Esters of Azaspiracids Identified in Mussels (*Mytilus edulis*) using Liquid**

2   **Chromatography-High Resolution Mass Spectrometry**

3

4   Elizabeth M. Mudge, Christopher O. Miles, William R. Hardstaff, Pearse McCarron*

5

6   Biotoxin Metrology, National Research Council Canada, 1411 Oxford St., Halifax, Nova Scotia,
7   B3H 3Z1, Canada

8   *Corresponding Author:

9   Phone: +1 (902) 426-6182

10 Email: Pearse.McCarron@nrc-cnrc.gc.ca

11

1 **ABSTRACT**

2 Azaspiracids (AZAs) are lipophilic polyether toxins produced by *Azadinium* and *Amphidoma*

3 species of marine microalgae. The main dinoflagellate precursors AZA1 and AZA2 are

4 metabolized by shellfish to produce an array of AZA analogues. Using liquid chromatography-

5 high resolution mass spectrometry, fatty acid esters of AZAs with hydroxy groups at C-3 and C-

6 23 were confirmed in mussels (*Mytilus edulis*) contaminated with AZAs. The structures of these

7 acyl derivatives were determined through mass spectrometry experiments, and supported by

8 periodate cleavage reactions and semi-synthesis of palmitate esters of the AZAs. Esters of the

9 hydroxy groups at C-20 or C-21 were not observed in mussel tissue. The relative proportion of

10 the most abundant AZA ester (3-*O*-palmitoylAZA4) was less than 3% of the sum of the major free

11 AZA analogues in the hepatopancreas tissue. These findings reveal an additional metabolic

12 pathway for AZAs in shellfish.

13 **Keywords:** azaspiracid, fatty acid, ester, LC-HRMS, shellfish, metabolism, mussel

14

1. INTRODUCTION

Since the first azaspiracid (AZA) poisoning event in 1995 from mussels (*Mytilus edulis*) harvested at Killary Harbour, Ireland, over 60 AZA analogs have been detected in shellfish and in *Amphidoma* and *Azadinium* spp. (Krock et al., 2019; Twiner et al., 2008). Azaspiracids have become a global concern, with *Azadinium* spp. and AZA-contaminated shellfish being detected in Europe, South America, North America, Australasia and Asia (Kim et al., 2017; Smith et al., 2016; Tillmann et al., 2016; Tillmann et al., 2009; Tillmann et al., 2017). AZA structures are characterized by three main functional groups: a cyclic amine, a tri-spiro assembly and a carboxylic acid. Two of the regulated analogues, AZA1 and -2, are produced by *A. spinosum*, while many others are shellfish metabolites and products from oxidation, hydroxylation, decarboxylation and dehydration (Figure 1) (Hess et al., 2014; Kilcoyne et al., 2015a; Kilcoyne et al., 2018; McCarron et al., 2009; Tillmann et al., 2009).
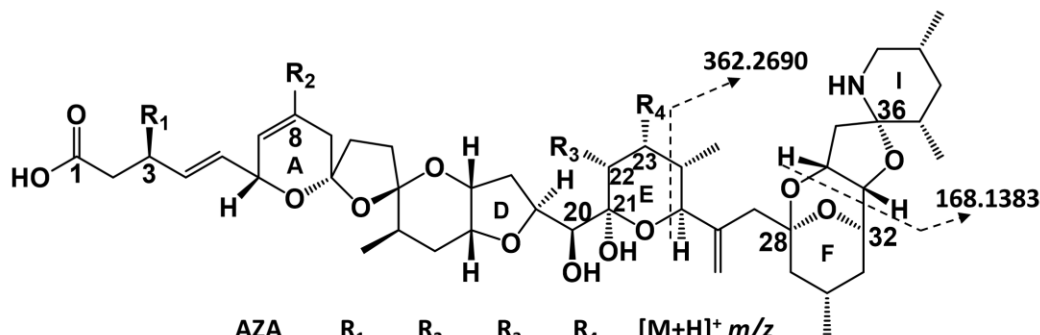
AZA	R$_1$	R$_2$	R$_3$	R$_4$	[M+H]$^+$ m/z
AZA1	H	H	CH$_3$	H	842.5049
AZA2	H	CH$_3$	CH$_3$	H	856.5206
AZA3	H	H	H	H	828.4893
AZA4	OH	H	H	H	844.4842
AZA5	H	H	H	OH	844.4842
AZA6	H	CH$_3$	H	H	842.5049
AZA7	OH	H	CH$_3$	H	858.4998
AZA8	H	H	CH$_3$	OH	858.4998
AZA9	OH	CH$_3$	H	H	858.4998
AZA10	H	CH$_3$	H	OH	858.4998
AZA11	OH	CH$_3$	CH$_3$	H	872.5155
AZA12	H	CH$_3$	CH$_3$	OH	872.5155
AZA13	OH	H	H	OH	860.4791
AZA14	OH	H	CH$_3$	OH	874.4947
AZA15	OH	CH$_3$	H	OH	874.4947
AZA16	OH	CH$_3$	CH$_3$	OH	888.5104

1

2   **Figure 1.** Structures of AZA1–16 and their protonated exact masses.

3   These lipophilic toxins accumulate in shellfish tissues and in addition to the mechanisms

4   described above have the potential to be metabolized similarly to other lipophilic toxin classes.

5   The documentation of fatty acid acyl esters of okadaic acid, dinophysistoxins, pectenotoxins,

6   brevetoxins, spirolides, pinnatoxins and gymnodimines highlights the potential for acylation of

7   hydroxy groups to form esters and higher toxicity than indicated by the analysis of free toxins

8   (Aasen et al., 2006; de la Iglesia et al., 2013; McCarron et al., 2012; Morohashi et al., 1995;

9   Torgersen et al., 2008; Wilkins et al., 2006). The majority of AZAs in shellfish, especially those

10   metabolized from AZA1 or -2, contain C-20 and C-21 hydroxy groups, while hydroxy groups can

1   also be present at C-3 and C-23 (Figure 1). The presence of these hydroxy groups presents the

2   potential for acyl ester formation of AZAs in shellfish. The regulatory limit of 160 µg/kg AZA1 eq.

3   set by the European Commission applies to free AZA1–3, which were the first AZAs identified in

4   shellfish, while other analogues are generally observed at lower concentrations (European

5   Commission, 2011; Hess et al., 2014). To date, *in vitro* potencies are reported as AZA2 > AZA6 >

6   AZA34 ≈ 37-*epi*-AZA1 > AZA8 ≈ AZA3 > AZA1 > AZA4 ≈ AZA9 > AZA5 ≈ AZA10 > AZA33 > AZA26

7   (Kilcoyne et al., 2014a; Kilcoyne et al., 2018; Kilcoyne et al., 2014b; Kilcoyne et al., 2015b; Krock

8   et al., 2015; Twiner et al., 2012).

9   AZA fatty acid esters were not detected in previous studies of mussel tissues (Rehmann

10   et al., 2008). However, synthetic acylation reactions have shown that AZA1 can undergo fatty

11   acid esterification (de la Iglesia et al., 2014). We herein report the use of liquid chromatography-

12   high resolution mass spectrometry (LC-HRMS) for the detection of AZA fatty acid esters in mussel

13   (*M. edulis*) tissues. The backbone AZA structures of these esters were verified based on product

14   ion spectra, periodate cleavage experiments, and through comparison to semi-synthetic AZA acyl

15   esters.

16

17   **2.   MATERIALS AND METHODS**

18   **2.1.   Chemicals and Reagents**

19   LC-MS grade acetonitrile, methanol, ethanol, formic acid (~98 %) and reagent grade ethyl

20   acetate and hexane were from Fisher Scientific (Ottawa, ON, Canada). MS grade ammonium

21   formate (>99%), HPLC grade pyridine (99.9%), reagent grade sodium periodate (>99%), 4-

22   dimethylaminopyridine (DMAP, >98%), palmitic anhydride (99%) and sodium chloride were from

1   Millipore-Sigma (Oakville, ON, Canada). Distilled water was ultra-purified to 18.2 MΩ·cm using a

2   Milli-Q water purification system (Millipore-Sigma, Billerica, MA, USA).

3   AZA1 calibration solution and mussel (*M. edulis*) matrix certified reference materials

4   (CRM-AZA1b, CRM-AZA-Mus and CRM-FDMT1) were from the National Research Council Canada

5   (Halifax, NS, Canada). In-house reference materials for AZA4, -7 and -9 were prepared as

6   described previously (Kilcoyne et al., 2015b). Mussel (*M. edulis*) tissues contaminated with AZAs

7   provided by the Marine Institute, Ireland, were collected from the following locations: Killary

8   Harbour, 1995; Bruckless, Donegal Bay, Sept. 2005; and Gouladoo, Bantry Bay, 2008.

9   **2.2.   Sample Preparation**

10   The hepatopancreas (HP) tissue of mussels containing AZAs from Bruckless was dissected

11   from a subset of the mussels, homogenized and stored at −20 °C. Tissues from Killary Harbour

12   and Gouladoo were homogenized whole mussel tissues stored at −20 °C prior to analysis.

13   Homogenized tissue (2 g) was extracted with MeOH (4 mL) by vortex mixing for 1 min and

14   centrifuged at 3950 *g* for 5 min. The supernatant was decanted into a 10 mL volumetric flask, the

15   pellet was re-extracted with an additional 4 mL of MeOH, centrifuged as above, and the

16   supernatants were combined in the volumetric flask and made to volume with MeOH. An aliquot

17   of the extract was filtered (0.2 µm Teflon spin-filter; Millipore-Sigma) prior to analysis.

18   **2.3.   AZA Ester Fraction Preparation**

19   Dissected HP (150 g) from Bruckless mussels was freeze-dried to yield 40 g of dry tissue,

20   which was extracted with EtOH (3 × 100 mL) in a Waring blender. The extract was filtered

21   (Whatman no. 5 filter paper) and evaporated under vacuum at 35 °C. The residue was partitioned

22   between EtOAc (150 mL) and 1.0 M NaCl (100 mL). The fractions from each step of the procedure

1   were analyzed by LC-MS to verify the presence of AZAs and AZA-esters. The EtOAc fraction was

2   evaporated under vacuum and the residue partitioned between hexane (50 mL) and 90% MeOH

3   (50 mL). The methanolic fraction was evaporated under vacuum. The residue was applied to an

4   open silica gel column (10 cm × 5.0 cm i.d.) packed with 10-40 µm silica gel (Millipore-Sigma) and

5   sequentially eluted with hexane–EtOAc (9:1), EtOAc–MeOH (7:3 and 1:1), and MeOH (250 mL

6   each). The 7:3 and 1:1 EtOAc–MeOH fractions were evaporated under vacuum separately, and

7   dissolved in MeOH (10 mL) for analysis.

8   **2.4.   LC-HRMS**

9   Analyses were performed on an Agilent 1200 LC equipped with a binary pump,

10   temperature controlled autosampler and column compartment coupled to a Q Exactive HF

11   Orbitrap mass spectrometer (Thermo Fischer Scientific, Waltham, MA, USA) with a heated

12   electrospray ionization probe (HESI-II). The chromatographic separation used a C8 column (100

13   × 2.1, 1.9 µm Thermo Hypersil Gold; Thermo Fischer Scientific, Waltham, MA, USA) with gradient

14   elution. The mobile phase was water (A) and 95% MeCN (B), both containing 50 mM formic acid

15   and 2 mM ammonium formate. The elution gradient (0.25 mL/min) was: 0–5 min, 50-100% B; 5–

16   20 min, 100% B; 20–20.1 min, 100–50% B; and 5 min re-equilibration at 50% B. The column and

17   sample compartments were maintained at 20 °C and 10 °C, respectively. The injection volume

18   was 3 µL. The MS was calibrated from m/z 74–1622 according to the manufacturer's specification

19   using the positive Pierce LTQ Velos calibration solution (Thermo-Fisher Scientific). Full scan data

20   were collected from m/z 650–1200 using positive ionization with a spray voltage of 3.0 kV. The

21   sheath and auxiliary gas flows were 35 and 10, respectively. The capillary temperature was 350

1 °C and the heater temperature was 300 °C. The MS resolution setting was 60 000 with an AGC

2 target of 1×10^6 and a maximum injection time of 200 ms.

3 Data-independent acquisition (DIA) was used to screen for AZA-esters. Fifteen mass

4 windows of 39 Da spanned the range from m/z 650–1200 with stepped collision energies of 35

5 and 65 eV to collect product ion spectra from all ions within each window (Table S1). The MS

6 resolution was set at 15 000 with an AGC target of 2×10^5 and a maximum injection time of 50

7 ms with a loop count of 8.

8 Data-dependent acquisition (DDA) was used to collect MS/MS product ion scans of the

9 five most abundant ions in the full scan acquisition at each cycle, with an inclusion list for

10 candidate AZA-esters from the DIA acquisition. The mass range for full scan acquisition was m/z

11 950–1200 with a resolution setting of 60 000, an AGC target of 1×10^6 and maximum injection

12 time of 100 ms. Product ion scans were acquired with an isolation window of 1 m/z with stepped

13 collision energies of 35 and 65 eV. The resolution was set to 30 000 with an AGC target of 1×10^5

14 and a maximum injection time of 50 ms.

15 **2.5.   Semi-synthesis of palmitoylAZAs**

16 Palmitic acid (16:0) esters of AZA1, -4, -7 and -9 were prepared using a procedure

17 modified from previous applications to other algal toxins (Aasen et al., 2006; McCarron et al.,

18 2012). All glassware used was dried in a desiccator overnight prior to sample preparation.

19 Approximately 100 pmol of the individual AZA in MeOH was evaporated under nitrogen gas and

20 placed in a desiccator for 4 h to remove residual water. The residue was dissolved in 100 µL of

21 dry pyridine containing 30 mM palmitic anhydride and 100 mM DMAP. The solution was mixed

1 at room temperature and allowed to stand for 30 min. The pyridine was dried under nitrogen

2 and reconstituted in 100 μL of MeOH prior to LC-HRMS analysis.

3 **2.6.   Treatment with Sodium Periodate**

4 An aliquot (20 μL) of the semi-synthetic 3-*O*-palmitoylAZA4 in MeOH (20 μL) was mixed

5 with sodium periodate (50 mM, 2 μL) in an HPLC vial insert. An aliquot (20 μL) of the Bruckless

6 HP extract was mixed with 50 mM sodium periodate (2 μL) in another HPLC vial insert. These

7 solutions were vortex-mixed for 30 s and analyzed within 2 h by LC-HRMS.

8

9 **3.   RESULTS AND DISCUSSION**

10 **3.1.   Detection of AZA fatty acid esters**

11 Mussels collected from Bruckless, Ireland, in 2005 have previously been used for the

12 isolation of AZA analogues, and for the production of reference materials (Hess et al., 2007;

13 Kilcoyne et al., 2015a; Kilcoyne et al., 2015b; McCarron et al., 2015). Given that AZAs are sensitive

14 to the base hydrolysis conditions typically used for indirect analysis of fatty acid esters (Alfonso

15 et al., 2008), the Bruckless mussels were evaluated for intact fatty acid esters. To assist in the

16 detection of potentially low levels of AZA esters, HP tissues were analysed initially to provide a

17 more highly concentrated sample for LC-HRMS analysis. After elution of known AZAs, the

18 chromatographic separation was held at a high percentage organic mobile phase for 15 min to

19 elute non-polar compounds. The samples were screened by LC-HRMS for AZA fatty acid esters

20 using a DIA method which generated product ion scans from all ions within mass windows of

21 width *m/z* 39, from *m/z* 650 to 1200, to determine the approximate mass range and potential

1   precursor ions responsible for product ions characteristic of AZAs. The MS/MS fragmentation of

2   AZAs has previously been evaluated in detail, where many AZA analogues have the same

3   structural configuration towards the amino terminus, with characteristic product ions of *m/z*

4   362.2690 and 168.1383 resulting from fragmentation of the E and I rings, respectively (Figure 1)

5   (Rehmann et al., 2008). Given that there are no available hydroxy groups for known AZAs on this

6   part of the molecule (C-24 to C-40), putative AZA fatty acid esters should also fragment to give

7   these product ions. These two diagnostic ions were extracted from the DIA acquisition with a

8   mass error of 5 ppm, which confirmed the known AZA analogues eluting in the first 7 min, while

9   several later-eluting peaks also produced these characteristic AZA product ions (Figure 2). These

10   product ions from the later-eluting peaks were observed in the windows ranging from *m/z* 1052

11   to 1165.
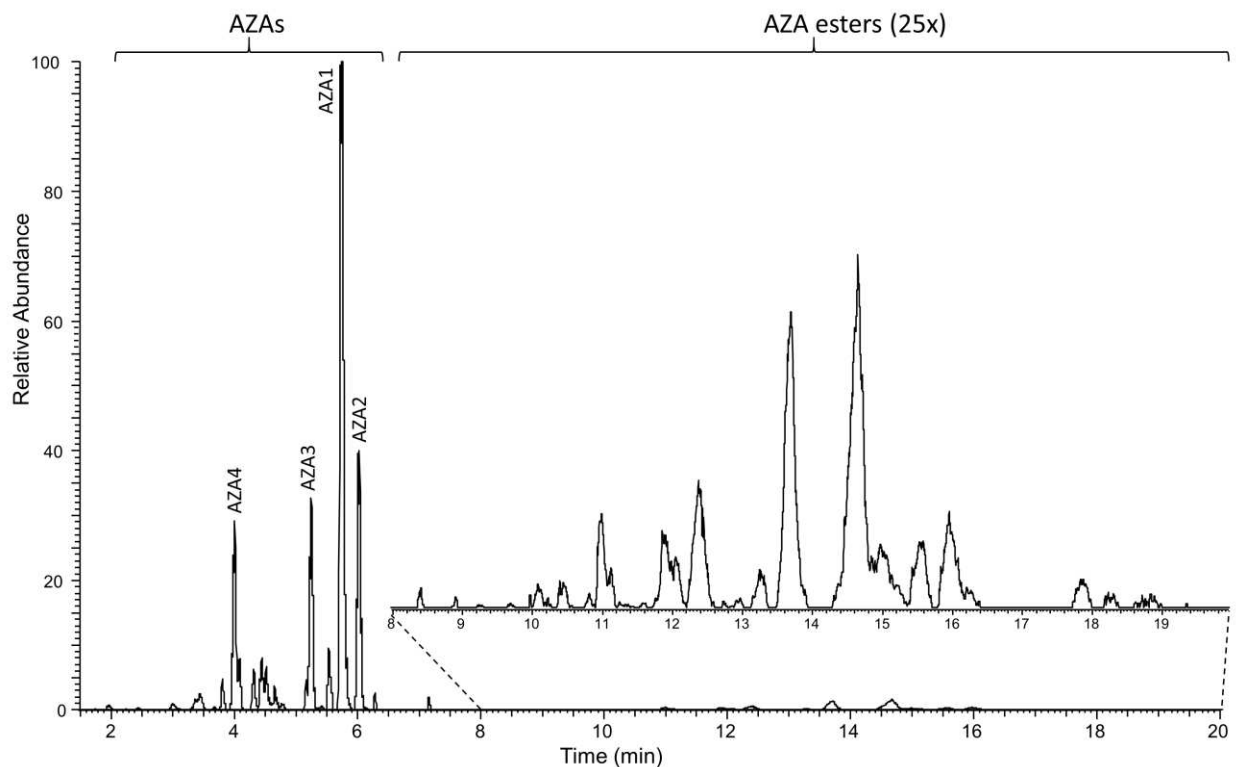
Figure 2. Sum of the extracted AZA diagnostic product ions at m/z 362.2690 and 168.1381 using a 5 ppm mass tolerance from the mass range of m/z 650 to 1250 collected using DIA acquisition of the HP extract of mussels collected from Bruckless.

To facilitate MS characterisation of these low-level AZA metabolites, an extract of the Bruckless mussel HP was fractionated and concentrated using silica gel chromatography (Kilcoyne et al., 2012). These fractions were used in targeted MS/MS experiments. The two most prominent peaks giving the diagnostic AZA product ions, eluting between 13–15 min (Figure 2), had a pseudomolecular ion $[M+H]^+$ of m/z 1082.7145, consistent with $C_{62}H_{100}O_{14}N^+$ (Δ 0.6 ppm). These two peaks had identical product ion spectra (Figure 3a,b). As is typical for AZAs, there was a series of water losses from the pseudomolecular ion. The m/z 808.4629 product ion ($C_{46}H_{66}O_{11}N^+$, -0.2 Δ ppm) is consistent with neutral loss of palmitic acid (hexadecanoic) and one molecule of water, suggesting the originally metabolized AZA would have a $[M+H]^+$ of m/z 844.4842 ($C_{46}H_{70}O_{13}N^+$) prior to forming a palmitate ester (16:0). The product ion at m/z 782.4845

1   ($C_{45}H_{68}O_{10}N^+$, Δ 0.9 ppm) is consistent with neutral loss of the fatty acid together with elimination

2   of C-1 as CO_2. Two ions that provided additional structural information on the AZA backbone

3   were m/z 658.3943 ($C_{37}H_{56}O_9N^+$, Δ −1.0 ppm) arising from retro-Diels–Alder cleavage of the A-

4   ring plus loss of water, and m/z 448.3049 ($C_{26}H_{42}O_5N^+$, Δ −1.9 ppm) from cleavage of C-19–C-20

5   with loss of water (Figure 4). These product ions, in addition to the m/z 808.4630 ion, are

6   characteristic of AZA4 (Rehmann et al., 2008), and strongly suggest that the two peaks arose from

7   3-*O*-palmitoyl AZA4. The identical fragmentation patterns of these two peaks suggests that the

8   location of acylation was the same, in addition to the backbone structure of this compound. The

9   presence of two peaks suggests a variation in the fatty acid chain (e.g. branching) or

10   epimerization in the AZA backbone that is not distinguishable by mass spectrometry, as has been

11   observed in other fatty acid esters (McCarron et al., 2012; Torgersen et al., 2008).

1
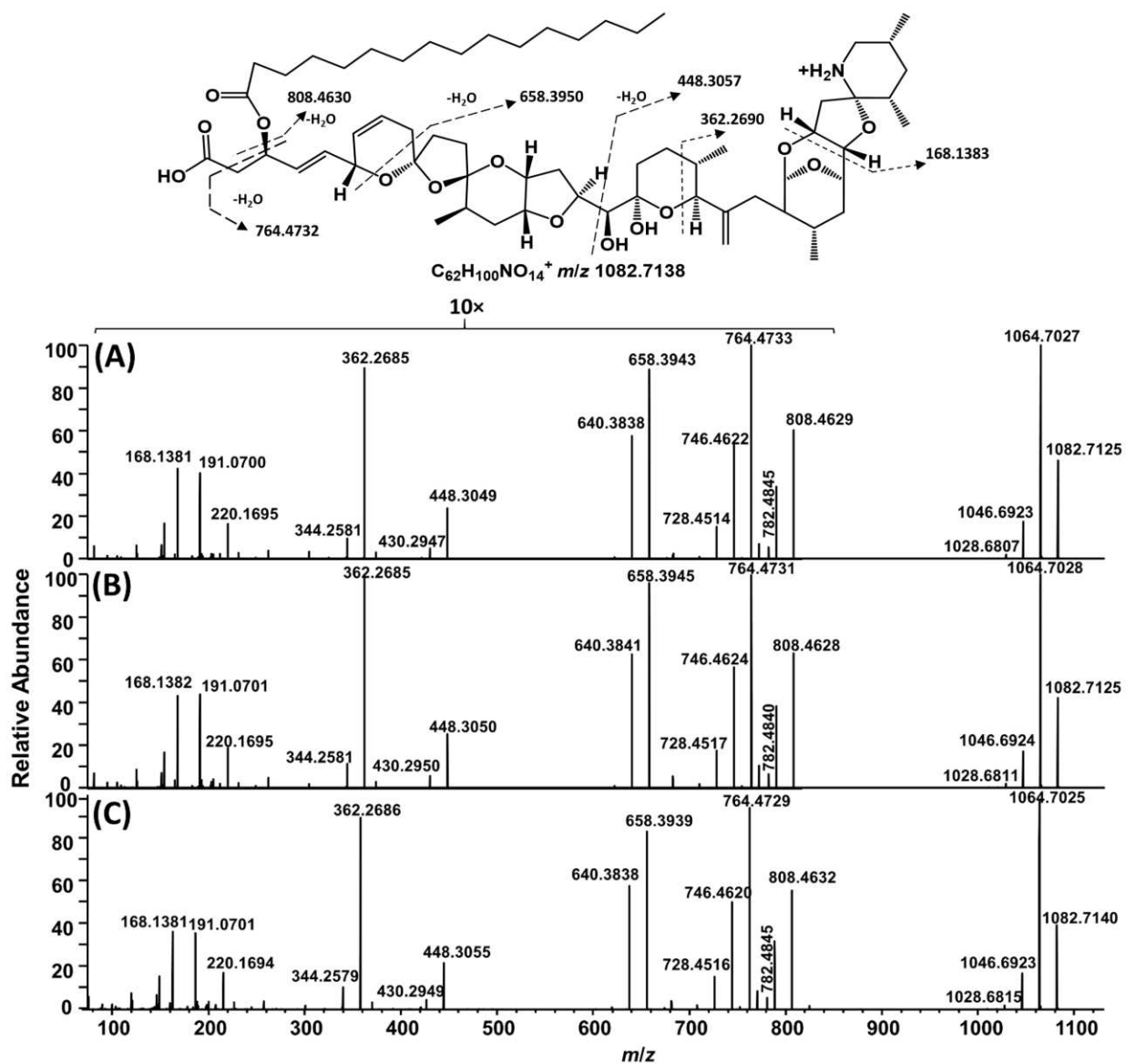
Figure 3. Extracted product ion spectra of (a,b) the two most abundant AZA-ester peaks using DDA acquisition in the fractionated HP of mussels collected in Bruckless. Both peaks arise from precursor ions at m/z 1082.7138 and the product ions are consistent with semi-synthetic 3-*O*-palmityolAZA4 (c) with a scheme showing the proposed origins of the major diagnostic ions with exact masses. The vertical scale from m/z 100–950 was expanded 10-fold to highlight diagnostic ions.

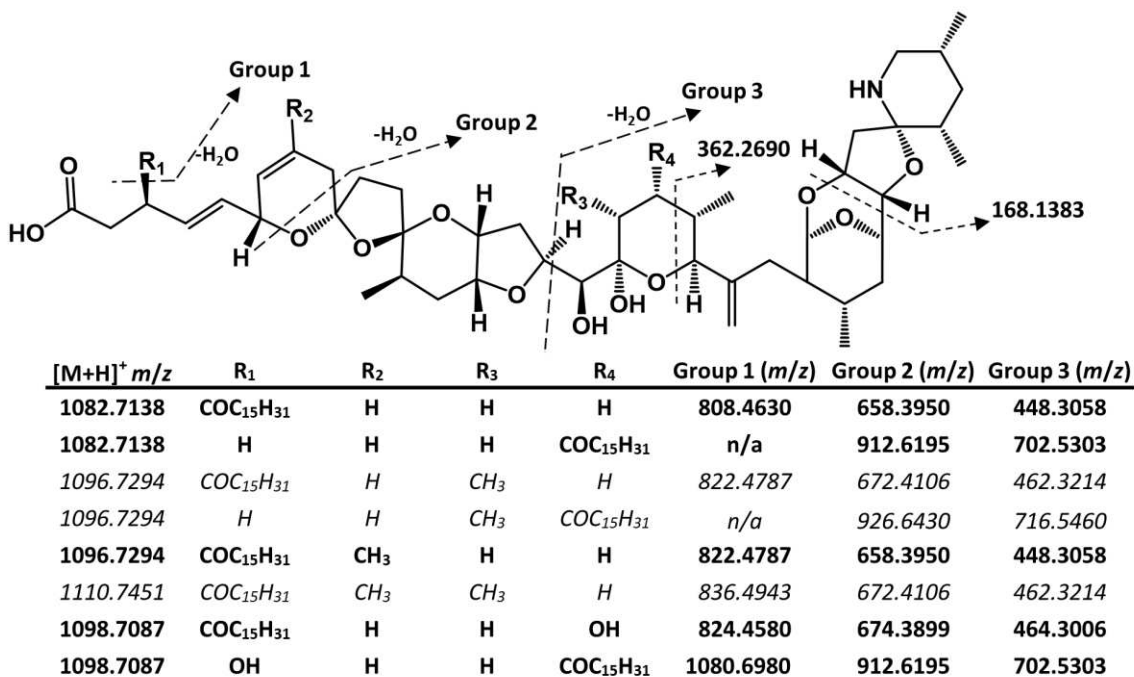The 3-*O*-palmitoyl AZA4 was synthesized by acylation of AZA4 with palmitic anhydride.

The acylation reaction was performed at room temperature where AZA4 reacted readily with

1   palmitic anhydride. The AZA4 peak area was reduced by 80% after 30 min, producing two main

2   products. The first product had an $[M+H]^+$ at m/z 826.4743 ($C_{46}H_{68}O_{12}N^+$, Δ 0.8 ppm) (Figure S1)

3   corresponding to dehydration of AZA4, and a second later-eluting product with $[M+H]^+$ at m/z

4   1082.7158 ($C_{62}H_{100}O_{14}N^+$, Δ 1.8 ppm) corresponding to 3-O-palmitoylAZA4. The retention time of

5   the semi-synthetic AZA4 palmitic acid ester was identical to the later-eluting 3-O-palmitoylAZA4

6   peak in the Bruckless sample (Figure S2). The Bruckless sample product ion spectra is consistent

7   with the proposed structure and identical to that of the semi-synthetic compound (Figure 3c),

8   confirming that these peaks are acyl esters of AZAs.

9   Previous quantitative analysis has shown that AZA4 is the most abundant of the non-

10   regulated AZAs in the Bruckless HP (McCarron et al., 2015). Table 1 summarizes the observed

11   AZA4 esters detected in the HP tissue based on exact mass and the presence of three diagnostic

12   AZA4 fragments (m/z 808.4630, 658.3950 and 448.3058). The most significant were consistent

13   with 16:0, 18:1, 16:1, 17:0, 20:2 and 18:0 3-O-acyl esters, based on peak area, which is consistent

14   with the fatty acid ester profiles observed for other acylated marine algal toxins in mussel tissues

15   (Aasen et al., 2006; de la Iglesia et al., 2013; McCarron et al., 2012; Torgersen et al., 2008).

16   The regulated AZA1–3 analogues contain free hydroxy groups on C-20 and C-21 (Figure

17   1), while AZA4 has an additional hydroxy group on C-3. Exact mass searches were negative for

18   fatty acid esters of the regulated AZAs, such as the 16:0 acyl ester of AZA1 ($[M+H]^+$ m/z

19   1080.7346), in the HP tissue, suggesting that the C-20 and C-21 hydroxyl groups are resistant to

20   esterification with fatty acids in mussels, possibly due to steric hindrance. Several additional AZAs

21   are hydroxylated at C-3, including AZA7, -9, -11, -13, while AZA5, -8 and -13 possess C-23 hydroxy

22   groups that could also undergo fatty acid esterification.

1   To determine identities of the other AZA esters present in the Bruckless HP tissue,

2   calculated MS/MS product ions for palmitate esters of the C-3 and C-23 hydroxylated AZAs were

3   generated (Figure 4) based on (Rehmann et al., 2008) and used as a basis for identification. The

4   fragments labelled as Groups 1–3 are diagnostic for the various acylated AZAs. Fatty acid esters

5   were observed for AZA9, with trace levels of AZA5 and AZA13 esters also detected. After AZA4,

6   the AZA9 fatty acid esters were most abundant.

	$[M+H]^+$ m/z	R_1	R_2	R_3	R_4	Group 1 (m/z)	Group 2 (m/z)	Group 3 (m/z)
AZA4	1082.7138	$COC_{15}H_{31}$	H	H	H	808.4630	658.3950	448.3058
AZA5	1082.7138	H	H	H	$COC_{15}H_{31}$	n/a	912.6195	702.5303
AZA7	*1096.7294*	*$COC_{15}H_{31}$*	*H*	*CH_3*	*H*	*822.4787*	*672.4106*	*462.3214*
AZA8	*1096.7294*	*H*	*H*	*CH_3*	*$COC_{15}H_{31}$*	*n/a*	*926.6430*	*716.5460*
AZA9	1096.7294	$COC_{15}H_{31}$	CH_3	H	H	822.4787	658.3950	448.3058
AZA11	*1110.7451*	*$COC_{15}H_{31}$*	*CH_3*	*CH_3*	*H*	*836.4943*	*672.4106*	*462.3214*
AZA13	1098.7087	$COC_{15}H_{31}$	H	H	OH	824.4580	674.3899	464.3006
AZA13	1098.7087	OH	H	H	$COC_{15}H_{31}$	1080.6980	912.6195	702.5303

7

8   **Figure 4.** Potential palmitate (16:0) acyl esters of azaspiracids containing 3- and 23-hydroxy groups and
9   the exact masses of their respective products ions used to screen the HRMS data. Note that no esters of
10   AZA7, -8 and -11 were detected in the HP tissue extract, and these entries are shown in italics.

11   The diagnostic product ions m/z 822.4780 ($C_{47}H_{68}O_{11}N^+$, Δ −0.8 ppm), 658.3945

12   ($C_{37}H_{56}O_9N^+$, Δ −0.7 ppm) and 448.3056 ($C_{26}H_{42}O_5N^+$, Δ −0.3 ppm) were used for identification of

13   the principal AZA9 fatty acid esters present (Table 1; Figure 5c). The majority of the other AZA

14   esters observed were present in low abundance relative to the AZA4 esters. The most abundant

15   acyl ester peak for each AZA in the HP tissue extract were the palmitate (16:0) esters. The mass

1   spectra for AZA4, -5, -9 and -13 palmitate esters (Figure 5) detected in the HP tissue each

2   displayed the diagnostic ions depicted in Figure 4.

3   **Table 1.** Accurate masses (for [M+H]$^+$), retention times and abundances (relative percentage to 3-*O*-
4   palmitoylAZA4) of AZA4 and AZA9 fatty acid acyl esters in the Bruckless mussel HP tissue.

AZA	Fatty Acid	C:DB[a]	Retention Time (min)	Peak Area Relative to 3-*O*-palmitoylAZA4 (%)	Neutral Molecular Formula	Accurate Mass	Δ (ppm)
	Tetradecaenoic	14:1	10.0	1.8	$C_{60}H_{93}O_{14}N$	1052.6671	0.2
	Tetradecanoic	14:0	12.0	8.1	$C_{60}H_{95}O_{14}N$	1054.6846	2.0
	Pentadecanoic	15:0	13.2	5.7	$C_{61}H_{97}O_{14}N$	1068.7003	2.0
	Hexadecatetraenoic	16:4	8.9	1.7	$C_{62}H_{91}O_{14}N$	1074.6544	2.9
	Hexadecadienoic	16:2	9.5	5.7	$C_{62}H_{95}O_{14}N$	1078.6840	1.4
	Hexadecaenoic	16:1	12.3	19.1	$C_{62}H_{97}O_{14}N$	1080.7000	1.7
	Hexadecanoic[b]	16:0	14.7	100.0	$C_{62}H_{99}O_{14}N$	1082.7159	1.9
	Heptadecaenoic	17:1	13.6	6.3	$C_{63}H_{99}O_{14}N$	1094.7146	0.7
	Heptadecanoic[b]	17:0	15.9	12.3	$C_{63}H_{101}O_{14}N$	1096.7318	2.1
	Octadecatetraenoic	18:4	9.9	3.1	$C_{64}H_{95}O_{14}N$	1102.6862	3.3
AZA4	Octadecatrienoic	18:3	11.1	1.0	$C_{64}H_{97}O_{14}N$	1104.7001	1.7
	Octadecadienoic	18:2	12.7	3.3	$C_{64}H_{99}O_{14}N$	1106.7160	2.0
	Octadecaenoic[b]	18:1	15.6	20.2	$C_{64}H_{101}O_{14}N$	1108.7315	1.8
	Octadecanoic[b]	18:0	17.9	9.8	$C_{64}H_{103}O_{14}N$	1110.7471	1.8
	Eicosapentaenoic	20:5	10.4	3.0	$C_{66}H_{97}O_{14}N$	1128.7006	2.1
	Eicosatetraenoic	20:4	11.8	0.7	$C_{66}H_{99}O_{14}N$	1130.7136	−0.2
	Eicosadienoic	20:2	15.9	10.8	$C_{66}H_{103}O_{14}N$	1134.7475	2.1
	Eicosenoic	20:1	18.9	5.9	$C_{66}H_{105}O_{14}N$	1136.7626	1.6
	Docosahexaenoic	22:6	10.9	7.1	$C_{68}H_{99}O_{14}N$	1154.7168	2.6
	Docosapentaenoic	22:5	12.4	2.0	$C_{68}H_{101}O_{14}N$	1156.7310	1.3
	Docosadienoic	22:2	19.3	4.9	$C_{68}H_{107}O_{14}N$	1162.7778	1.2
	Tetradecanoic	14:0	12.7	5.7	$C_{61}H_{97}O_{14}N$	1068.6971	−1.0
	Pentadecanoic	15:0	14.0	1.9	$C_{62}H_{99}O_{14}N$	1082.7153	1.4
	Hexadecaenoic	16:1	13.0	5.5	$C_{63}H_{99}O_{14}N$	1094.7146	0.7
AZA9	Hexadecanoic[b]	16:0	15.5	7.6	$C_{63}H_{101}O_{14}N$	1096.7314	1.7
	Heptadecanoic	17:0	17.0	0.5	$C_{64}H_{103}O_{14}N$	1110.7446	−0.5
	Octadecaenoic[b]	18:1	16.5	2.2	$C_{65}H_{103}O_{14}N$	1122.7440	−1.0
	Docosahexaenoic	22:6	11.5	1.1	$C_{69}H_{101}O_{14}N$	1168.7315	1.7

5   [a] carbons:desaturation
6   [b] Two peaks were observed with identical product ion spectra. RT is reported for the second peak, peak
7   areas were combined for the two, Δ <3 ppm for the first peak.
8   Note: Retention times of free AZA4 and AZA9 were 3.92 and 4.22 min, respectively
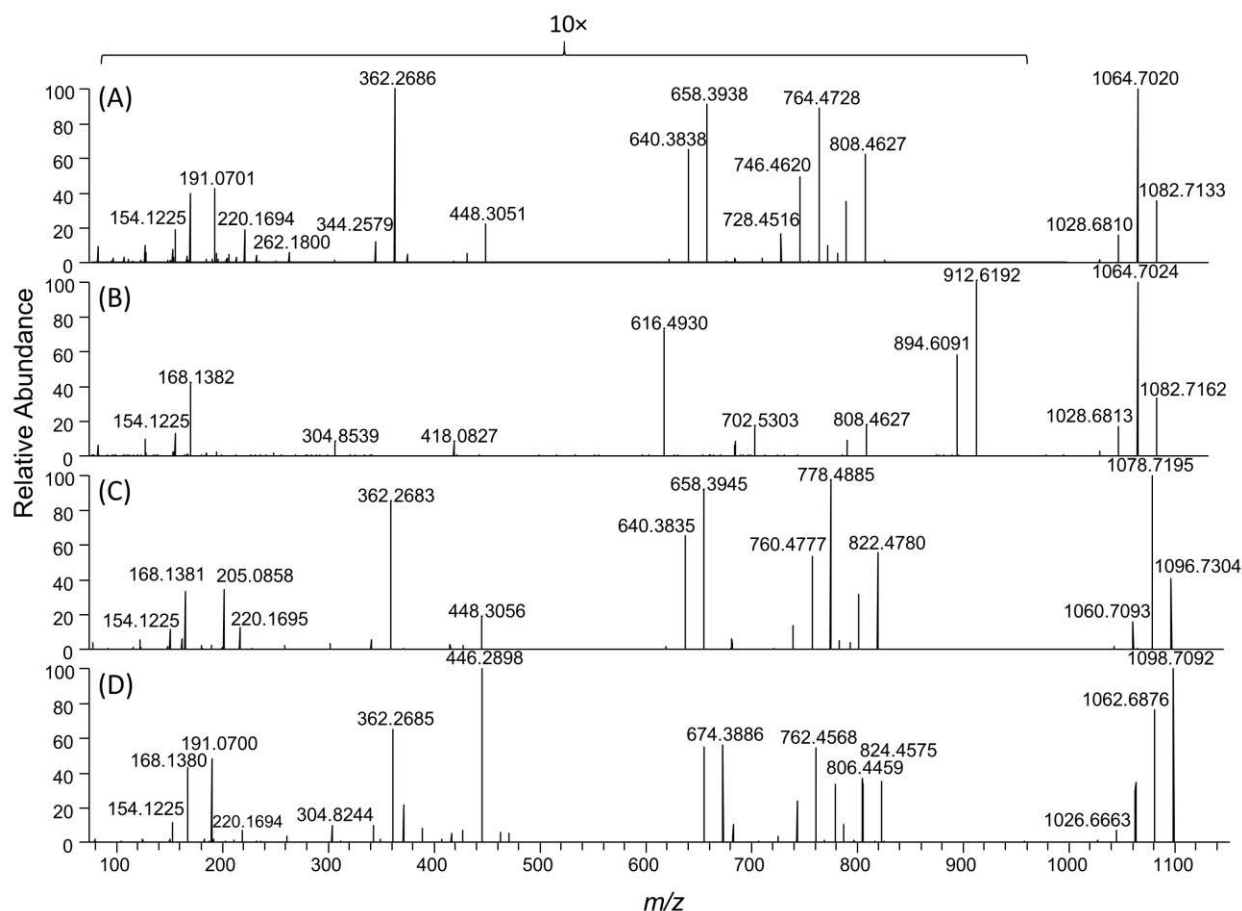
Figure 5. Product ion spectra of palmitate (16:0) acyl esters of: (a) AZA4; (b) AZA5; (c) AZA9, and; (d) AZA13, obtained using DDA acquisition of the fractionated mussel hepatopancreas from Bruckless. The vertical scale from m/z 100–950 was expanded 10-fold to highlight diagnostic ions.

A very low abundance peak with m/z 1082.7134 ($C_{62}H_{100}O_{14}N^+$, Δ −0.4 ppm) having product ions with m/z 912.6192 ($C_{53}H_{86}O_{11}N^+$, Δ −0.4 ppm) and m/z 702.5303 ($C_{42}H_{72}O_7N^+$, Δ −0.04 ppm) was consistent with palmitate esterification of the 23-hydroxy group of AZA5 (23-O-palmitoylAZA5; Figure 5c). This was the only AZA5 fatty acid ester observed in the HP tissues. Given the low relative abundance of this peak (ca 0.5% of 3-O-palmitoylAZA4), the metabolic pathway for esterification of AZA5, presumably for the 23-OH, appears to not be favoured in the mussels. However, the lower relative abundance of AZA5 compared to AZA4 in these tissues is also a consideration. The concentrations of AZA5 and AZA9 are both about four times lower than

17

1 AZA4 in the Bruckless tissue (McCarron et al., 2015) suggesting that 23-OH esterification in the

2 case of AZA5 is disfavoured. Esters of AZA8 and -11 were not detected in the HP tissue nor in the

3 concentrated fractions obtained from the silica gel fractionation. This suggests that the methyl

4 group on C-22 reduces the reactivity of 23-OH of AZAs toward fatty acids *in vivo*.

5 AZA13 contains hydroxy groups at both C-3 and C-23. Acyl esters for both of the 3- and

6 23-hydroxy groups of AZA13 were observed at very low levels in the HP tissue, consistent with

7 the low levels of free AZA13 in the source tissues with a pseudomolecular ion of *m/z* 1098.7102

8 ($C_{62}H_{102}O_{15}N^+$, Δ 1.3 ppm). Trace levels of 3-*O*-palmitoylAZA13 are evident by the presence of

9 product ions at *m/z* 824.4575, 674.3886, and 464.3015 ($C_{46}H_{66}O_{12}N^+$, Δ −0.6 ppm, $C_{37}H_{56}O_{10}N^+$, Δ

10 −1.9 ppm, and $C_{26}H_{42}O_6N^+$, Δ 1.8 ppm, respectively; Figure 5d, Figure S3), while the presence of

11 23-*O*-palmitoylAZA13 was confirmed by the observation of product ions at *m/z* 912.6197

12 ($C_{53}H_{86}O_{11}N^+$, Δ 0.2 ppm), *m/z* 824.4568 ($C_{46}H_{66}O_{12}N^+$, Δ −1.4 ppm) and *m/z* 702.5288 ($C_{42}H_{72}O_7N^+$,

13 Δ −2.2 ppm; Figure S3). Doubly acylated AZAs were not observed when a higher mass range was

14 investigated, although these would be more hydrophobic and may not elute under the

15 chromatographic conditions used here.

16 Trace levels of 3-*O*-palmitoylAZA7 were detected in the 7:3 EtOAC:MeOH silica gel

17 fraction, co-eluting with 3-*O*-margaroylAZA4 based on the observed product ions of *m/z*

18 822.4797, 672.4112 and 462.3218 ($C_{47}H_{68}O_{11}N^+$, Δ 1.2 ppm, $C_{38}H_{58}O_9N^+$, Δ 0.9 ppm, and

19 $C_{27}H_{44}O_5N^+$, Δ 0.9 ppm, respectively; Figure S4).

3.2. Further comparison with synthetic palmitoylAZAs

The acylation reaction between palmitic anhydride and AZA9 resulted in a peak with identical retention time to the later-eluting of the two 3-O-palmitoylAZA9 peaks in the mussel HP tissue. The product ion spectrum (Figure S5) was also identical with that observed for the same peak in the Bruckless sample. Acylation of AZA7 with palmitic anhydride also produced a peak with a product ion spectrum matching that expected for 3-O-palmitoylAZA7 (Figure S6), confirming that it is possible to synthetically produce esters of this analogue.

Previously, semi-synthetic preparation of 16:0 AZA1 was successful using three different acylation routes (de la Iglesia et al., 2014). The location of the fatty acid was not confirmed, but the authors suggested that it occurred at the hydroxy group at C-20 due to that location being less sterically hindered. Acylation of AZA1 with palmitic anhydride was performed in this work using a method similar to one used by de la Iglesia (2014) except that the reaction was performed at room temperature rather than at 75 °C. The majority of AZA1 (approx. 70%) remained intact after reaction at room temperature (Figure S7), but a small peak of palmitoylAZA1 was generated with m/z 1080.7355 ($C_{63}H_{102}O_{13}N^+$, 0.9 Δ ppm) and retention time of 13.3 min, which was not present in the tissue extracts. The product ion spectrum confirmed acylation on the C-20 or C-21 hydroxy group via a characteristic product ion at m/z 928.6499 ($C_{54}H_{90}O_{11}N^+$, Δ −1.0 ppm) along with other AZA1 diagnostic product ions (Figure S7). Given that fatty acid esters of AZAs without C-3 or C-23 hydroxy groups were not detected in mussels in this study, despite free AZA1–3 and -6 typically being among the major AZAs in the samples, suggests that the C-20 and C-21 hydroxy groups may be unreactive toward *in vivo* enzymatic acylation. These data highlight the

1   importance of comparing products of synthetic reactions with authentic naturally-incurred

2   materials to verify their identities and biological significance.

3   **3.3.   Treatment of mussel extract and semi-synthetic 3-*O*-palmitoylAZA4 with NaIO₄**

4   Sodium periodate-mediated oxidative cleavage reactions provided additional structural

5   information on the AZA esters. The 20,21-diol present in most AZAs can be oxidatively cleaved

6   with periodate, and this reaction has been used as a tool in structure elucidation of novel AZAs

7   (Kilcoyne et al., 2014a; Kilcoyne et al., 2018; Kilcoyne et al., 2014b; Rehmann et al., 2008).

8   However, AZAs containing fatty acid esters on C-20 or C-21 would not be expected to undergo

9   the cleavage reaction with periodate, given that there would no longer be a 1,2-diol present at

10   C-20 and C-21. The semi-synthetic 3-*O*-palmitoylAZA4 reacted completely with periodate within

11   2 h, providing additional confirmation that esterification took place on the C-3 hydroxyl, and not

12   on the C-20 hydroxyl. The AZA esters in the Bruckless extract were also cleaved by periodate,

13   confirming that the esters present *in vivo* formed via reaction with either the C-3 or C-23 hydroxy

14   group, while the C-20 and C-21 hydroxy groups had not been esterified, possibly due to steric

15   hindrance or enzyme specificity (Figure S8).

16   **3.4.   Presence of AZA esters in CRMs and other tissues**

17   Additional mussel tissues and reference materials were evaluated for the presence of

18   fatty acid esters of AZA. As noted, the Bruckless mussel tissues analysed in this study were used

19   in the preparation of two CRMs (CRM-AZA-Mus and CRM-FDMT1). Consequently, the presence

20   of AZA fatty acid esters in these reference materials provides positively-characterized materials

21   that are available for use in other studies. 3-*O*-palmitoylAZA4 and 3-*O*-oleoylAZA4 (the 16:0 and

22   18:1 esters, respectively) were detected in all samples evaluated. CRM-FDMT1 and CRM-AZA-

1 Mus (McCarron et al., 2015; McCarron et al., 2017) contained trace levels of additional AZA4 fatty

2 acid esters (Table S2), primarily those that had a peak area relative to 3-*O*-palmitoylAZA4 ratio of

3 >10% in the Bruckless sample (Table 1). The content of 3-*O*-palmitoylAZA4 was estimated based

4 on the peak areas of its $[M+H]^+$ ion in full scan mode relative to that of AZA4 in the certified

5 tissues assuming the same molar response factor, and is summarized in Table 2. These semi-

6 quantitative estimates indicate approximate levels ranging from 0.005–0.03 mg/kg of tissue in

7 fresh whole mussel homogenates, with higher concentrations in the freeze-dried and HP tissues

8 at 0.15 mg/kg. This represents 0.2 to 2.5% of the total free AZA1–4 concentrations by weight in

9 the tissues. The mussels from Killary Harbour that were implicated in the original AZA poisoning

10 event (Satake et al., 1998) contained only 3-*O*-palmitoyl- and 3-*O*-oleoylAZA4 at trace levels,

11 while the mussel sample from Gouladoo, Bantry Bay, contained a higher content of AZA4 3-*O*-

12 acyl esters including 10 different acyl moieties, similar to those observed in high abundance in

13 the Bruckless HP, as well as 3-*O*-palmitoylAZA-9.

14 **Table 2.** Estimated concentrations of AZA1–4 and 3-*O*-palmitoylAZA4 (i.e. 16:0 esters) in several AZA-
15 incurred tissues assuming equivalent molar response to AZA4.

Tissue Sample	Concentration (mg/kg)				
	AZA1	AZA2	AZA3	AZA4	16:0 AZA4*
FDMT1[†]	4.10 ± 0.40	1.13 ± 0.10	0.96 ± 0.10	0.42 ± 0.01	0.15 ± 0.01
CRM-AZA-mus[†]	1.16 ± 0.10	0.27 ± 0.02	0.21 ± 0.02	0.17 ± 0.01	0.02 ± 0.01
HP tissue (Bruckless, 2005)	2.85 ± 0.11	1.36 ± 0.06	1.34 ± 0.04	0.36 ± 0.02	0.15 ± 0.01
Gouladoo (2012)	3.64 ± 0.01	1.26 ± 0.04	0.60 ± 0.02	0.15 ± 0.01	0.03 ± 0.01
Killary (1995)	1.13 ± 0.12	0.39 ± 0.04	0.17 ± 0.02	0.07 ± 0.01	0.005 ± 0.001

16 * Calculated as AZA4 equivalents, [†] AZA1–3 concentrations and uncertainty based on certified values

17

18 Relative toxicities of AZAs based on *in vitro* assays have shown that methylation on C-22

19 increases toxicity, while hydroxylation on C-3 or C-23 reduces toxicity (Kilcoyne et al., 2018).

20 While the okadaic acid and dinophysistoxin acyl esters have lower toxicities relative to their free

1 toxins, there is limited information available on the toxicity of many acyl ester metabolites of

2 algal toxins in shellfish (Torgersen et al., 2005). The AZA fatty acid esters detected in Atlantic

3 European mussels in this work were of low relative abundance compared to the major free AZAs,

4 and were formed for C-3 or C-23 hydroxylated AZAs with only trace levels of esters for AZAs with

5 methylation at C-22, suggesting they are of reduced toxicological significance. However, further

6 work should investigate ester formation for other AZA analogues, as well as AZA ester distribution

7 across mussel tissues and variation across a larger sample set to determine species and location

8 differences. It should also be considered that AZA esters may undergo hydrolysis during

9 digestion, which presents a risk of exposure to higher levels of the toxins than predicted based

10 on the analysis of free toxins. Future investigations will require optimization of the semi-synthesis

11 reaction conditions for a broader range of AZAs in order to improve quantitative measurements

12 of AZA fatty acid esters and to provide toxicological information.

13   In mussel feeding studies with *A. spinosum,* AZA1–2 appeared within 6 h and remained at

14 relatively constant concentrations, while the concentration of total metabolites continued to

15 increase for the duration of the feeding experiments (Jauffrais et al., 2012a; Jauffrais et al.,

16 2012b; Salas et al., 2011). Acylation of okadaic acid has been shown to be involved in the

17 depuration of these toxins from shellfish (Rossignoli et al., 2011) and may have a similar function

18 with AZAs. Given that during shellfish feeding with *Azadinium* spp., AZA accumulation appears to

19 stabilize, there may be additional biotransformations such as *O*-acylation that could contribute

20 to an increase in total AZAs over time. Future studies evaluating the accumulation,

21 transformation and depuration of AZAs in shellfish should consider the significance of additional

22 metabolites such as fatty acid esters.

1

4.   CONCLUSIONS

The presence of AZA fatty acid esters was confirmed in mussel tissues using LC-HRMS/MS and chemical reactions. These hydrophobic metabolites elute after previously reported AZAs, but share common MS/MS fragmentation characteristics, with the majority of esters observed being formed from AZA4 or AZA9 with trace levels formed from AZA5, AZA7 and AZA13. The primary fatty acid involved in esterification was palmitic acid (16:0), which was confirmed based on semi-synthesis of 3-O-palmitoylAZA4. The discovery of these acyl esters highlights an additional metabolic pathway for AZAs in shellfish, and shellfish feeding studies would be important to study their accumulation, transformation and depuration kinetics. The methodologies employed here can be used to evaluate a broader range of AZA-incurred materials to compare ester profiles and the variation in esterification across different shellfish species.

13

1 **REFERENCES**

2 Aasen, J.A.B., Hardstaff, W., Aune, T., Quilliam, M.A., 2006. Discovery of fatty acid ester metabolites of
3 spirolide toxins in mussels from Norway using liquid chromatography/tandem mass spectrometry. Rapid
4 Commun. Mass Spectrom. 20, 1531−1537.

5 Alfonso, C., Rehmann, N., Hess, P., Alfonso, A., Wandscheer, C.B., Abuín, M., Vale, C., Otero, P., Vieytes,
6 M.R., Botana, L.M., 2008. Evaluation of various pH and temperature conditions on the stability of
7 azaspiracids and their importance in preparative isolation and toxicological studies. Anal. Chem. 80,
8 9672−9680.

9 de la Iglesia, P., Fonollosa, E., Diogène, J., 2014. Assessment of acylation routes and structural
10 characterisation by liquid chromatography/tandem mass spectrometry of semi-synthetic acyl ester
11 analogues of lipophilic marine toxins. Rapid Commun. Mass Spectrom. 28, 2605−2616.

12 de la Iglesia, P., McCarron, P., Diogène, J., Quilliam, M.A., 2013. Discovery of gymnodimine fatty acid
13 ester metabolites in shellfish using liquid chromatography/mass spectrometry. Rapid Commun. Mass
14 Spectrom. 27, 643−653.

15 European Commission, 2011. Commision Regulation (EU) No 15/2011 amending Regulation (EC) No
16 2074/2005 as regards recognised testing methods for detecting marine biotoxins in live bivalve
17 molluscs. Off. J. Euro. Union.

18 Hess, P., McCarron, P., Krock, B., Kilcoyne, J., Miles, C.O., 2014. Azaspiracids: Chemistry, biosynthesis,
19 metabolism, and detection, in: Botana, L.M. (Ed.), Seafood and Freshwater Toxins, 2nd ed. CRC Press,
20 Boca Raton, pp. 799−821.

21 Hess, P., McCarron, P., Rehmann, N., Kilcoyne, J., McMahon, T., Ryan, G., Ryan, P., Twiner, J.M.,
22 Doucette, G.J., Ito, E., Yasumoto, T., 2007. Isolation and purification of azaspiracids from naturally
23 contaminated materials, and evaluation of their toxicological effects– final project report ASTOX
24 (ST/02/02) Marine Institute – Marine Environment & Health Series.

25 Jauffrais, T., Contreras, A., Herrenknecht, C., Truquet, P., Séchet, V., Tillmann, U., Hess, P., 2012a. Effect
26 of *Azadinium spinosum* on the feeding behaviour and azaspiracid accumulation of *Mytilus edulis*. Aquat.
27 Toxicol. 124−125, 179−187.

28 Jauffrais, T., Marcaillou, C., Herrenknecht, C., Truquet, P., Séchet, V., Nicolau, E., Tillmann, U., Hess, P.,
29 2012b. Azaspiracid accumulation, detoxification and biotransformation in blue mussels (*Mytilus edulis*)
30 experimentally fed *Azadinium spinosum*. Toxicon 60, 582−595.

31 Kilcoyne, J., Keogh, A., Clancy, G., LeBlanc, P., Burton, I., Quilliam, M.A., Hess, P., Miles, C.O., 2012.
32 Improved isolation procedure for azaspiracids from shellfish, structural elucidation of azaspiracid-6, and
33 stability studies. J. Agric. Food Chem. 60, 2447−2455.

34 Kilcoyne, J., McCarron, P., Hess, P., Miles, C.O., 2015a. Effects of Heating on proportions of azaspiracids
35 1–10 in mussels (*Mytilus edulis*) and identification of carboxylated precursors for azaspiracids 5, 10, 13,
36 and 15. J. Agric. Food Chem. 63, 10980−10987.

1 Kilcoyne, J., McCarron, P., Twiner, M.J., Nulty, C., Crain, S., Quilliam, M.A., Rise, F., Wilkins, A.L., Miles,
2 C.O., 2014a. Epimers of azaspiracids: Isolation, structural elucidation, relative LC-MS response, and *in*
3 *vitro* toxicity of 37-*epi*-azaspiracid-1. Chem. Res. Toxicol. 27, 587−600.

4 Kilcoyne, J., McCarron, P., Twiner, M.J., Rise, F., Hess, P., Wilkins, A.L., Miles, C.O., 2018. Identification of
5 21,22-dehydroazaspiracids in mussels (*Mytilus edulis*) and *in vitro* toxicity of azaspiracid-26. J. Nat. Prod.
6 81, 885−893.

7 Kilcoyne, J., Nulty, C., Jauffrais, T., McCarron, P., Herve, F., Foley, B., Rise, F., Crain, S., Wilkins, A.L.,
8 Twiner, M.J., Hess, P., Miles, C.O., 2014b. Isolation, structure elucidation, relative LC-MS response, and
9 *in vitro* toxicity of azaspiracids from the dinoflagellate *Azadinium spinosum*. J. Nat. Prod. 77, 2465−2474.

10 Kilcoyne, J., Twiner, M.J., McCarron, P., Crain, S., Giddings, S.D., Foley, B., Rise, F., Hess, P., Wilkins, A.L.,
11 Miles, C.O., 2015b. Structure elucidation, relative LC–MS response and *in vitro* toxicity of azaspiracids 7–
12 10 isolated from mussels (*Mytilus edulis*). J. Agric. Food Chem. 63, 5083−5091.

13 Kim, J.-H., Tillmann, U., Adams, N.G., Krock, B., Stutts, W.L., Deeds, J.R., Han, M.-S., Trainer, V.L., 2017.
14 Identification of *Azadinium* species and a new azaspiracid from *Azadinium poporum* in Puget Sound,
15 Washington State, USA. Harmful Algae 68, 152−167.

16 Krock, B., Tillmann, U., Potvin, É., Jeong, J.H., Drebing, W., Kilcoyne, J., Al-Jorani, A., Twiner, J.M., Göthel,
17 Q., Köck, M., 2015. Structure elucidation and *in vitro* toxicity of new azaspiracids isolated from the
18 marine dinoflagellate *Azadinium poporum*. Mar. Drugs 13, 6687−6702.

19 Krock, B., Tillmann, U., Tebben, J., Trefault, N., Gu, H., 2019. Two novel azaspiracids from *Azadinium*
20 *poporum*, and a comprehensive compilation of azaspiracids produced by Amphidomataceae,
21 (Dinophyceae). Harmful Algae 82, 1−8.

22 McCarron, P., Giddings, S.D., Reeves, K.L., Hess, P., Quilliam, M.A., 2015. A mussel (*Mytilus edulis*) tissue
23 certified reference material for the marine biotoxins azaspiracids. Anal. Bioanal. Chem. 407, 2985−2996.

24 McCarron, P., Kilcoyne, J., Miles, C.O., Hess, P., 2009. Formation of azaspiracids-3, -4, -6, and -9 via
25 decarboxylation of carboxyazaspiracid metabolites from shellfish. J. Agric. Food Chem. 57, 160−169.

26 McCarron, P., Rourke, W.A., Hardstaff, W., Pooley, B., Quilliam, M.A., 2012. Identification of pinnatoxins
27 and discovery of their fatty acid ester metabolites in mussels (*Mytilus edulis*) from Eastern Canada. J.
28 Agric. Food Chem. 60, 1437−1446.

29 McCarron, P., Wright, E., Emteborg, H., Quilliam, M.A., 2017. A mussel tissue certified reference material
30 for multiple phycotoxins. Part 4: certification. Anal. Bioanal. Chem. 409, 95−106.

31 Morohashi, A., Satake, M., Murata, K., Naoki, H., Kaspar, H.F., Yasumoto, T., 1995. Brevetoxin B3, a new
32 brevetoxin analog isolated from the greenshell mussel *Perna canaliculus* involved in neurotoxic shellfish
33 poisoning in New Zealand. Tetrahedron Lett. 36, 8995−8998.

34 Rehmann, N., Hess, P., Quilliam, M.A., 2008. Discovery of new analogs of the marine biotoxin azaspiracid
35 in blue mussels (*Mytilus edulis*) by ultra-performance liquid chromatography/tandem mass
36 spectrometry. Rapid Commun. Mass Spectrom. 22, 549−558.

1 Rossignoli, A.E., Fernández, D., Regueiro, J., Mariño, C., Blanco, J., 2011. Esterification of okadaic acid in
2 the mussel *Mytilus galloprovincialis*. Toxicon 57, 712−720.

3 Salas, R., Tillmann, U., John, U., Kilcoyne, J., Burson, A., Cantwell, C., Hess, P., Jauffrais, T., Silke, J., 2011.
4 The role of *Azadinium spinosum* (Dinophyceae) in the production of azaspiracid shellfish poisoning in
5 mussels. Harmful Algae 10, 774−783.

6 Satake, M., Ofuji, K., Naoki, H., James, K.J., Furey, A., McMahon, T., Silke, J., Yasumoto, T., 1998.
7 Azaspiracid, a new marine toxin having unique spiro ring assemblies, isolated from Irish mussels, *Mytilus*
8 *edulis*. J. Am. Chem. Soc. 120, 9967−9968.

9 Smith, K.F., Rhodes, L., Harwood, D.T., Adamson, J., Moisan, C., Munday, R., Tillmann, U., 2016.
10 Detection of *Azadinium poporum* in New Zealand: The use of molecular tools to assist with species
11 isolations. J. Appl. Phycol. 28, 1125−1132.

12 Tillmann, U., Borel, C.M., Barrera, F., Lara, R., Krock, B., Almandoz, G.O., Witt, M., Trefault, N., 2016.
13 *Azadinium poporum* from the Argentine continental shelf, Southwestern Atlantic, produces azaspiracid-
14 2 and azaspiracid-2 phosphate. Harmful Algae 51, 40−55.

15 Tillmann, U., Elbrächter, M., Krock, B., John, U., Cembella, A., 2009. *Azadinium spinosum* gen. et sp. nov.
16 (Dinophyceae) identified as a primary producer of azaspiracid toxins. Eur. J. Phycol. 44, 63−79.

17 Tillmann, U., Trefault, N., Krock, B., Parada-Pozo, G., de la Iglesia, R., Vásquez, M., 2017. Identification of
18 *Azadinium poporum* (Dinophyceae) in the Southeast Pacific: morphology, molecular phylogeny, and
19 azaspiracid profile characterization. J. Plankton Res. 39, 350−367.

20 Torgersen, T., Aasen, J., Aune, T., 2005. Diarrhetic shellfish poisoning by okadaic acid esters from Brown
21 crabs (*Cancer pagurus*) in Norway. Toxicon 46, 572−578.

22 Torgersen, T., Wilkins, A.L., Rundberget, T., Miles, C.O., 2008. Characterization of fatty acid esters of
23 okadaic acid and related toxins in blue mussels (*Mytilus edulis*) from Norway. Rapid Commun. Mass
24 Spectrom. 22, 1127−1136.

25 Twiner, J.M., Rehmann, N., Hess, P., Doucette, J.G., 2008. Azaspiracid shellfish poisoning: A review on
26 the chemistry, ecology, and toxicology with an emphasis on human health impacts. Mar. Drugs 6, 39−72.

27 Twiner, M.J., El-Ladki, R., Kilcoyne, J., Doucette, G.J., 2012. Comparative effects of the marine algal
28 toxins azaspiracid-1, -2, and -3 on Jurkat T lymphocyte cells. Chem. Res. Toxicol. 25, 747−754.

29 Wilkins, A.L., Rehmann, N., Torgersen, T., Rundberget, T., Keogh, M., Petersen, D., Hess, P., Rise, F.,
30 Miles, C.O., 2006. Identification of fatty acid esters of pectenotoxin-2 seco acid in blue mussels (*Mytilus*
31 *edulis*) from Ireland. J. Agric. Food Chem. 54, 5672−5678.

32

Fatty Acid Esters of Azaspiracids Identified in Mussels (*Mytilus edulis*) using Liquid Chromatography-High Resolution Mass Spectrometry

Elizabeth M. Mudge, Christopher O. Miles, William R. Hardstaff, Pearse McCarron*

Biotoxin Metrology, National Research Council Canada, 1411 Oxford St., Halifax, Nova Scotia, B3H 3Z1, Canada

*Corresponding Author:

Phone: +1 (902) 426-6182

Email: Pearse.McCarron@nrc-cnrc.gc.ca

Supplementary Data

Table S1. Inclusion list for DIA acquisition with the mass centers for each of the 15 acquisition windows with a mass width of *m/z* 39, and the stepped collision energy (NCE).

Mass (*m/z*)	Polarity	NCE
668.0000	Positive	35, 65
705.0000	Positive	35, 65
742.0000	Positive	35, 65
778.0000	Positive	35, 65
815.0000	Positive	35, 65
852.0000	Positive	35, 65
888.0000	Positive	35, 65
925.0000	Positive	35, 65
962.0000	Positive	35, 65
998.0000	Positive	35, 65
1035.0000	Positive	35, 65
1072.0000	Positive	35, 65
1108.0000	Positive	35, 65
1145.0000	Positive	35, 65
1182.0000	Positive	35, 65

**Table S2.** Summary of 3-*O*-acyl AZA esters detected in whole mussel tissues. (+) detected, (-) not detected.

| Ester	CRM-FDMT1	CRM-AZA-Mus	Killary	Gouladoo
14:0 AZA4	+	+	-	+
15:0 AZA4	+	+	-	+
16:1 AZA4	+	+	-	+
16:0 AZA4	+	+	+	+
17:1 AZA4	+	+	-	+
17:0 AZA4	+	+	-	+
18:1 AZA4	+	+	+	+
18:0 AZA4	-	-	-	+
20:5 AZA4	-	-	-	+
20:2 AZA4	+	+	-	-
22:6 AZA4	-	+	-	+
16:0 AZA9	-	-	-	+
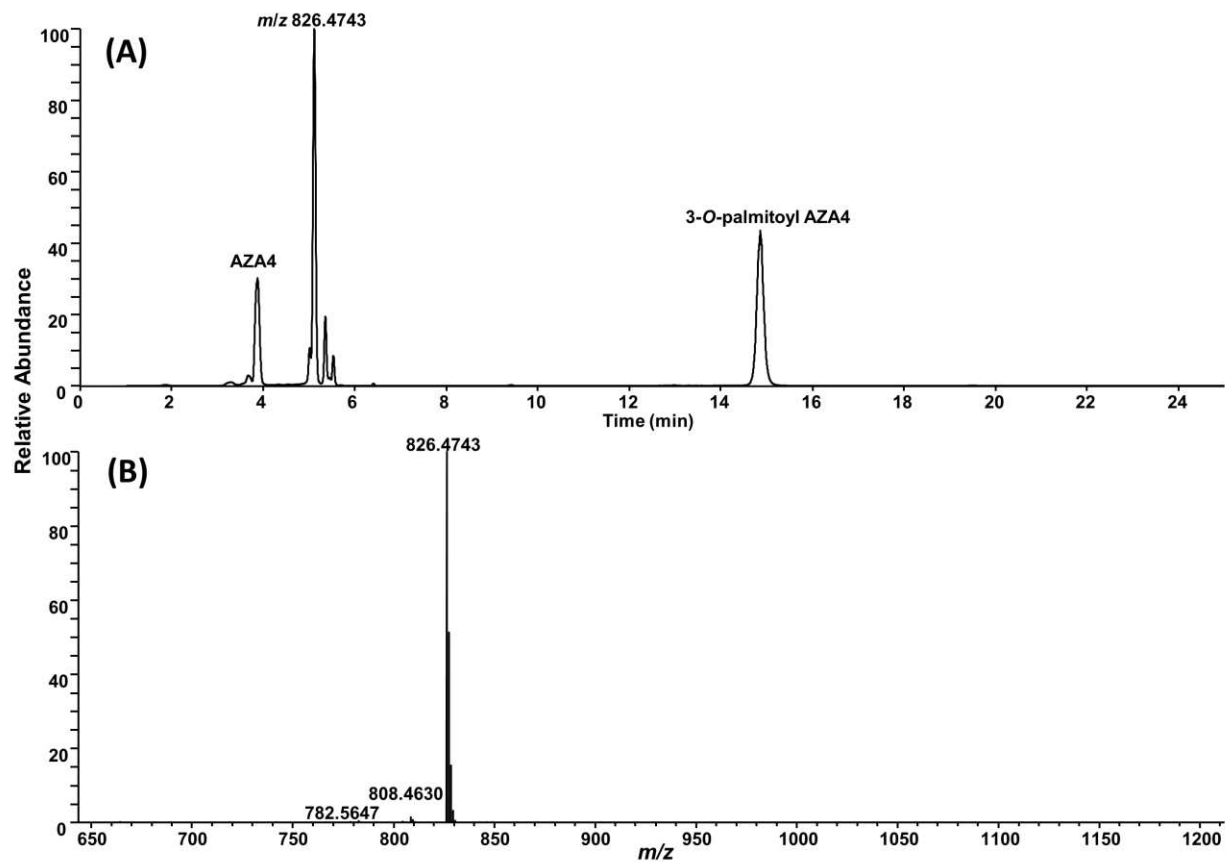
Figure S1. (A) Extracted ion chromatogram of AZA4, the product at *m/z* 826.4743 and 3-*O*-palmitoyl AZA4 from semi-synthesis of 3-*O*-palmitoyl (16:0) AZA-4. (B) Full scan MS spectrum of the product with [M+H]$^+$ of *m/z* 826.4743, suspected to be due to 2,3-dehydroAZA4 ($C_{46}H_{68}O_{12}N^+$, Δ 0.8 ppm) based on periodate cleavage of the 20,21-diol (data not shown).
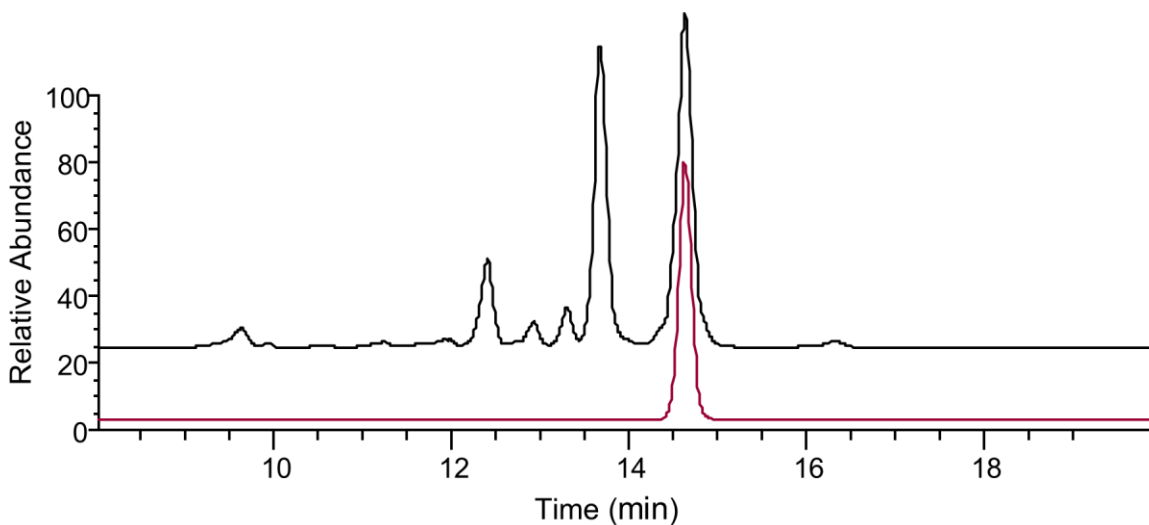
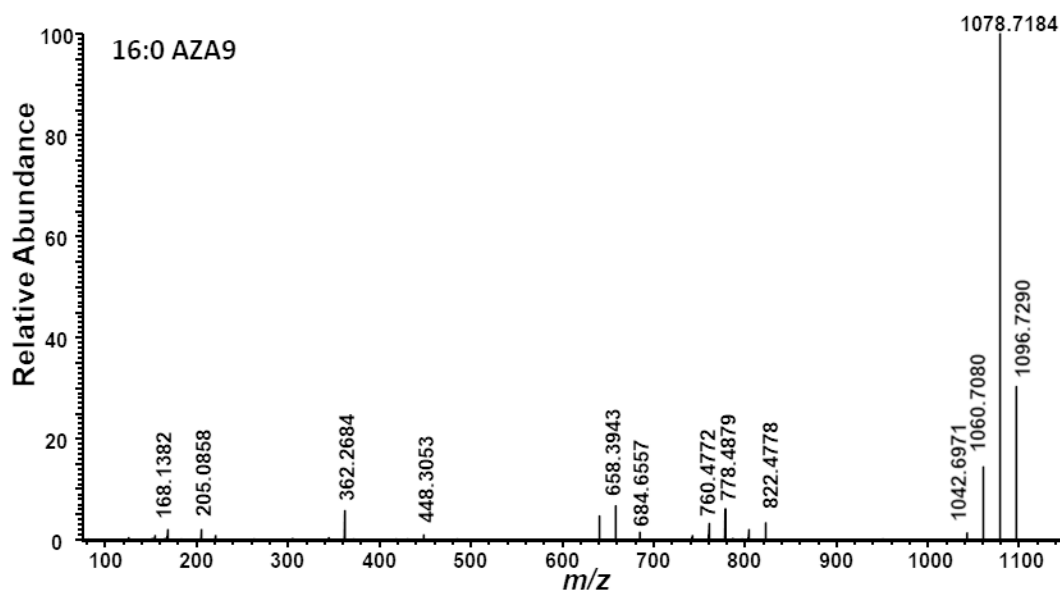**Figure S2.** Extracted ion chromatogram of *m/z* 1082.7138 (±5 ppm) of the Bruckless HP tissue (black) and the semi-synthesized 3-*O*-palmitoylAZA4 (red).
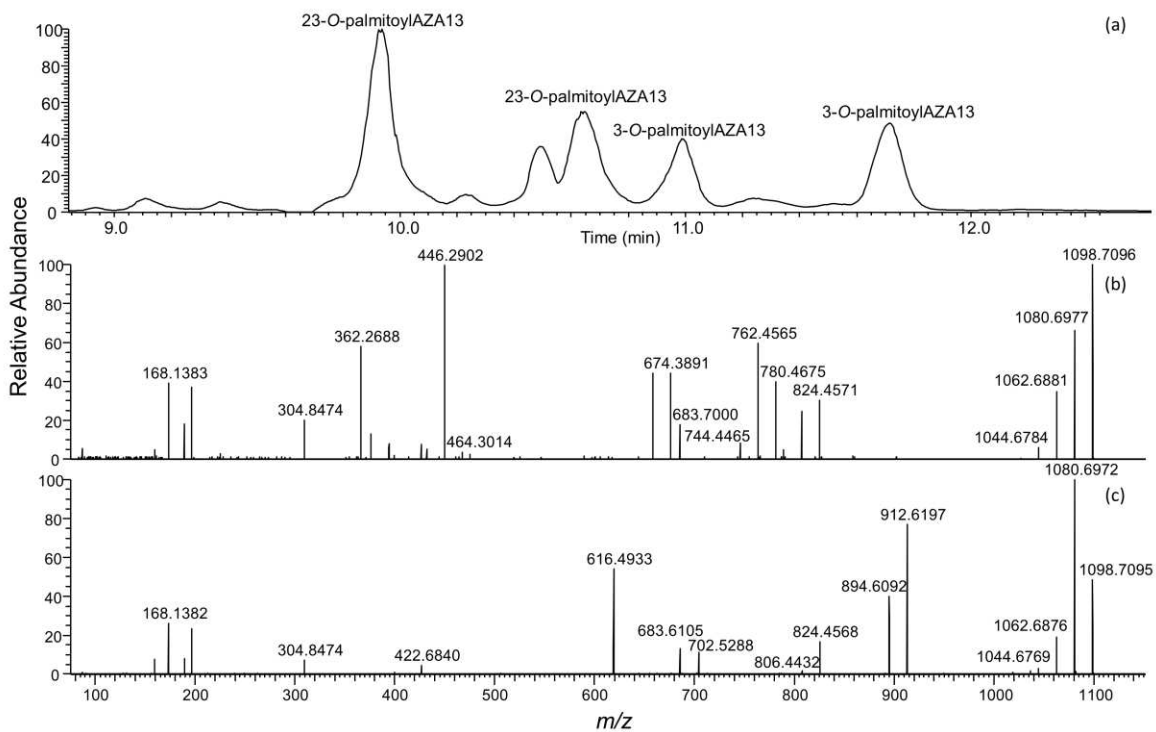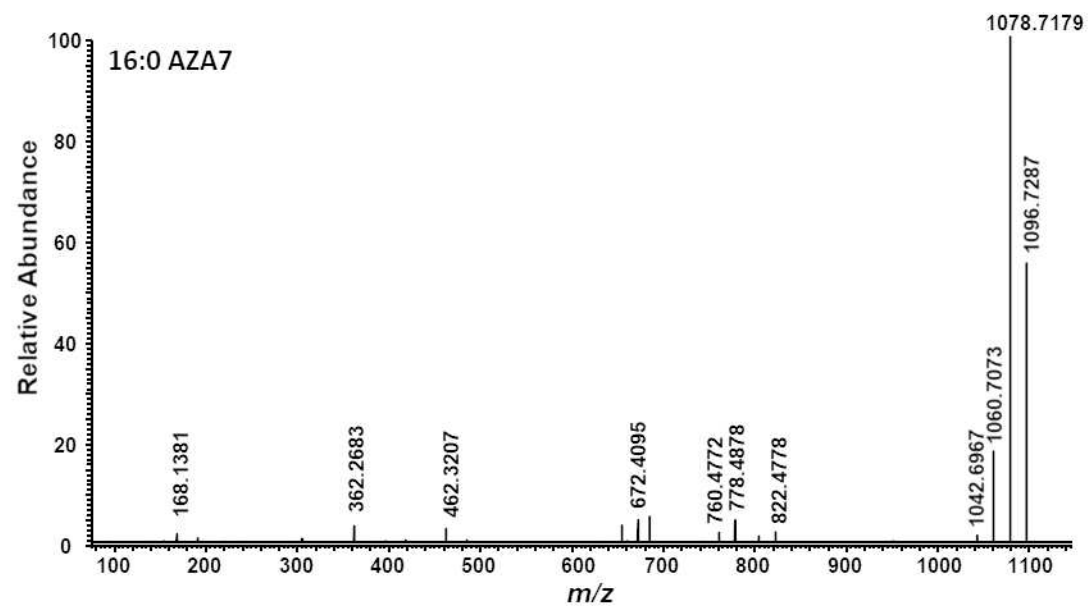

Figure S3. (a) Extracted ion chromatogram of *m/z* 1098.7087 (±5 ppm) for palmitate esters of AZA13 in the hepatopancreas mussel from Bruckless. Product ion spectrum of (b) 3-*O*-palmitoylAZA13, and (c) 23-*O*-palmitoylAZA13 observed in the HP tissue. The vertical scale from m/*z* 100- 950 was expanded 20× to highlight diagnostic ions.
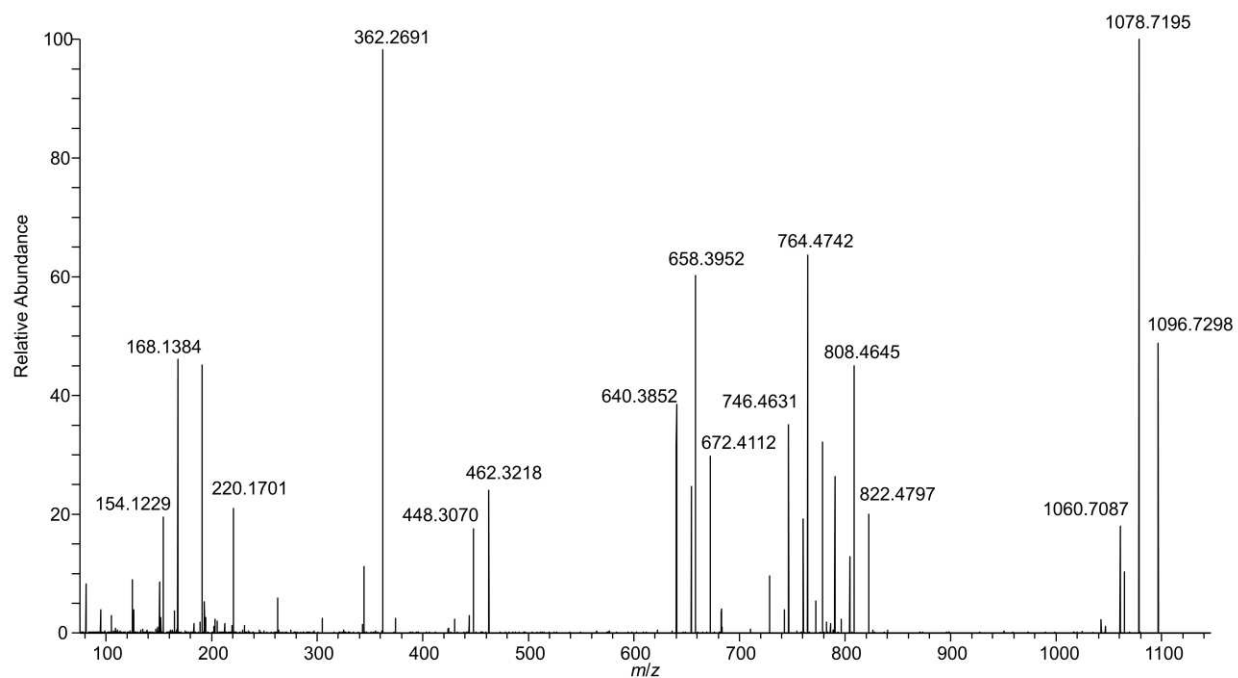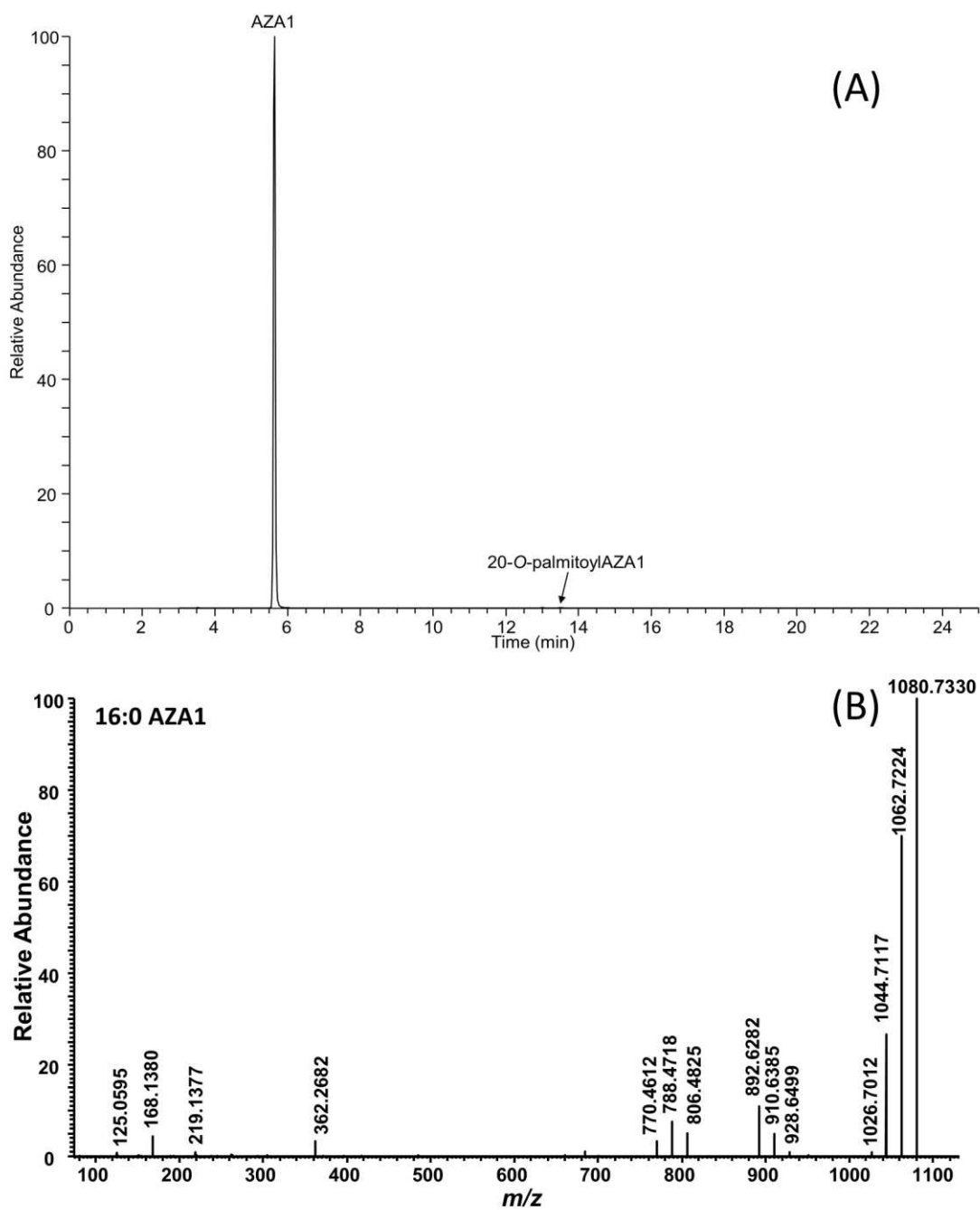
Figure S4. Product ion spectra of 3-*O*-pamitoylAZA7 co-eluting with 3-*O*-margaroylAZA4 in the concentrated 7:3 EtOAc:MeOH silica gel fraction of the hepatopancreas tissue. The vertical scale from *m/z* was expanded 20× to highlight diagnostic ions.


Figure S5. Product ion spectrum of semi-synthetic 3-*O*-palmitoylAZA9, which was confirmed to be present in the HP tissue.

Figure S6. Product ion spectrum of the semi-synthetic 3-*O*-palmitoylAZA7.

Figure S7. (A) Extracted ion chromatogram of AZA1 (*m/z* 842.5049) and of the semi-synthetic 16:0 ester of AZA1 (presumed to be 20-*O*-palmitoylAZA1, *m/z* 1080.7345) (B) Product ion spectrum of the semi-synthesized 20-*O*-palmitoylAZA1), which was not detected in the HP tissue.
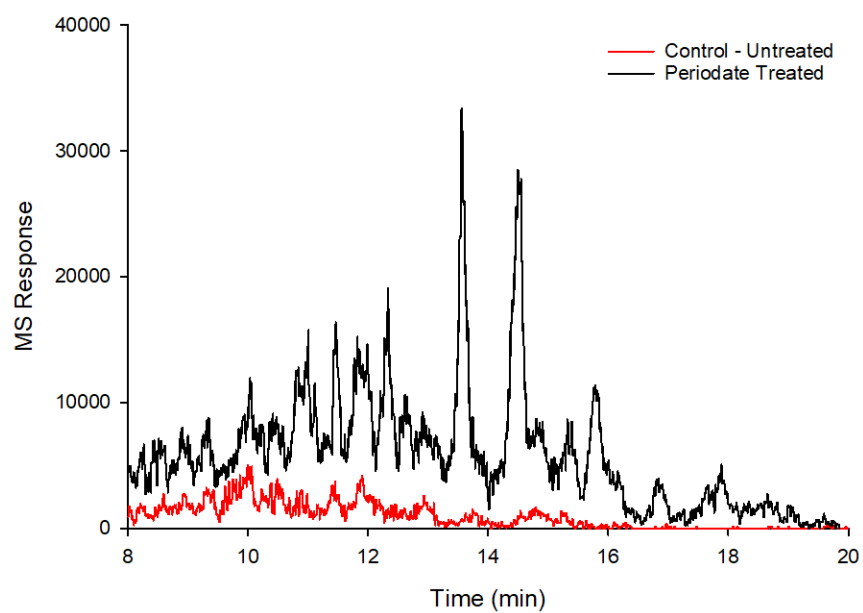
Figure S8. Extracted ion chromatogram of the product ions at *m/z* 362.2690 and 168.1381 from the mass range of *m/z* 650 to 1250 using DIA acquisition in the HP tissue in a control extract (black) and 2 h after treatment with sodium periodate.